

See discussions, stats, and author profiles for this publication at: <https://www.researchgate.net/publication/6343535>

Minimum Energy Pathways for Proton Transfer between Adjacent Sites Exposed to Water

ARTICLE in THE JOURNAL OF PHYSICAL CHEMISTRY B · JUNE 2007

Impact Factor: 3.3 · DOI: 10.1021/jp070781r · Source: PubMed

CITATIONS

14

READS

25

5 AUTHORS, INCLUDING:



Ran Friedman

Linnaeus University

31 PUBLICATIONS 587 CITATIONS

SEE PROFILE



Stefan Fischer

Universität Heidelberg

97 PUBLICATIONS 14,976 CITATIONS

SEE PROFILE



Esther Nachliel

Tel Aviv University

104 PUBLICATIONS 2,134 CITATIONS

SEE PROFILE



Menachem Gutman

Tel Aviv University

181 PUBLICATIONS 3,582 CITATIONS

SEE PROFILE

Minimum Energy Pathways for Proton Transfer between Adjacent Sites Exposed to Water

Ran Friedman,^{*,†,||} Stefan Fischer,[‡] Esther Nachliel,[†] Steve Scheiner,[§] and Menachem Gutman[†]

Laser Laboratory for Fast Reactions in Biology, Department of Biochemistry, Tel Aviv University, 69978 Ramat Aviv, Tel Aviv, Israel, IWR, University of Heidelberg, Im Neuenheimer Feld 368, D-69120 Heidelberg, Germany, and Department of Chemistry and Biochemistry, Utah State University, 300 Old Main Hill, Logan, Utah 84322-0300

Received: January 30, 2007

The capacity to transfer protons between surface groups is an innate property of many proteins. The transfer of a proton between donor and acceptor, located as far as 6–7 Å apart, necessitates the participation of water molecules in the process. In a previous study we investigated the mechanism of proton transfer (PT) between bulk exposed sites, a few ångströms apart, using as a model the proton exchange between the proton-binding sites of the fluorescein molecule in dilute aqueous solution.¹ The present study expands the understanding of PT reactions between adjacent sites exposed to water through the calculation the minimum energy pathways (MEPs) by the conjugate peak refinement algorithm² and a quantum-mechanical potential. The PT reaction trajectories were calculated for the fluorescein system with an increasing number of water molecules. The MEP calculations reveal that the transition state is highly strained and involves a supramolecular structure in which fluorescein and the interconnecting water molecules are covalently bonded together and the protons are shared between neighboring oxygens. These findings are in accord with the high activation energy, as measured for the reaction, and indicate that PT reactions on the surface proceed by a semi- or fully concerted rather than stepwise mechanism. A similar mechanism is assumed to be operative on the surface of proteins and renders water-mediated PT reactions as highly efficient as they are.

Introduction

Proton transfer through water is an essential step in electrochemical-biological energy conversion processes. In the mitochondria or chloroplasts, the protons compensate for electron-transfer reactions by permeating the biomembranes through specific pathways that transverse the enzymes involved in the reactions.^{3–6} The entry of a proton to a dedicated channel is preceded by its diffusion, both in bulk and on the surface, until encounter with the orifice of the channel takes place. High turnover proton pumping proteins, such as bacteriorhodopsin,^{7–9} F₀F₁ ATP synthase,¹⁰ photosynthetic reaction center,¹¹ and cytochrome c oxidase^{12–15} execute, during the catalytic cycle, proton transfer (PT) reactions at rates that exceed the velocity at which free proton can react with the active site. These proteins developed efficient proton-collecting antenna systems on their surfaces, utilizing clusters of carboxylates as proton attractor sites.^{13,16} These carboxylates act as proton donors and acceptors, forming a percolating network of proton-transferring moieties. The capacity to transfer protons between surface groups is an innate property of many proteins. This has recently been demonstrated by studies of PT on the surface of the S6 ribosomal protein, which is not a proton pumping protein.¹⁷ The flexibility of the surface, relative motion of the residues, and density of packing of protonable residues are all sufficient for PT.

In previous reports, we summarized our studies on PT reactions at the surface of fluorescein¹ and fluorescein deriva-

tives.¹⁸ These molecules were selected as models for the study of PT reactions on proteins with the advantage that advanced molecular modeling procedures could be performed. Fluorescein is a yellow fluorophore commonly used in medicine, biology, and chemistry. Its adsorption maxima, emission maxima, and isosbestic point are all in the visible wavelength. Fluorescein has two proton-binding sites, oxyanion and carboxylate, with pK_a's of 6.6 and 5.2, respectively. Protonation of the oxyanion modulates the spectral properties of the dye, while the carboxylate on the benzene ring has no effect on the chromophore. The distinction between these two sites enables the monitoring of the temporal states of their protonation. We could therefore follow the short-time protonation of fluorescein using the laser-induced proton pulse technique¹⁹ and analyze the PT reaction rates. By repeating the measurements at different temperatures, ionic strengths, and solvents (H₂O and D₂O), we could calculate the activation energy for the PT reaction on the surface of fluorescein, its salt sensitivity, and the kinetic isotope effect (KIE). The activation energy for the intramolecular proton-transfer reaction on fluorescein is as large as 11 kcal mol⁻¹. This value is ~3 times larger than the activation energy of proton diffusion in water. The PT reactions were found to be slower under high ionic strengths or in D₂O compared to reactions under low ionic strengths or in H₂O. In particular, we found a KIE of 50, which is unusually high compared to typical values for the KIE in intramolecular PT (1–6²⁰). To understand the peculiarity of this reaction, we investigated the dynamics of water molecules in the immediate vicinity of the dye by use of MD simulations. These simulations showed that the water molecules, which interconnect the donor and acceptor, create a highly ordered structure on the surface of fluorescein. This implies that the proton-transfer reactions on the surface of

* Author to whom correspondence should be addressed. Phone: +41-44-6355593. Fax: +41-44-6355521. E-mail: r.friedman@bioc.uzh.ch.

† Tel Aviv University.

‡ University of Heidelberg.

§ Utah State University.

|| Current Address: Department of Biochemistry, University of Zurich, Winterthurerstrasse 190, CH-8057 Zurich, Switzerland.

fluorescein are solvent-mediated and proceed through a chain of 2–5 water molecules that connect the donor and acceptor sites.

PT reactions on fluorescein have much in common with the reactions on the protein surface. First, the donor in fluorescein is a carboxyl, as in aspartate or glutamate protein residues. Second, the distance between the proton donor and acceptor is approximately 6 Å, similar to PT reactions on proteins (e.g., on the surface of bacteriorhodopsin²¹ or cytochrome c oxidase²²). Consequently, the rates of PT reactions on the surfaces of fluorescein and proteins are comparable, as are the reaction mechanisms.¹⁸ Understanding the peculiarities of the PT reactions on fluorescein can therefore shed light on PT reactions on proteins.

In the present study, we calculated the minimum energy pathway (MEP) for the PT reaction on the fluorescein surface, by use of the conjugate peak refinement (CPR) algorithm,² to find out whether the MEP is associated with high activation energy as determined experimentally (11 kcal mol⁻¹). MEPs were calculated using different numbers of interconnecting water molecules (1, 2, or 3). The calculations were repeated with larger numbers (up to 9) of water molecules to estimate the effect of solvation. Calculations of PT reactions necessitate the use of quantum-mechanical (QM) calculations due to the breaking and formation of covalent bonds. Accordingly, for the purpose of these calculations, the whole system was treated quantum mechanically. The energies were calculated by the use of the self-consistent charge density functional tight binding (SCC-DFTB) approximate density functional.^{23,24} This functional has been successfully used to study PT reactions^{25–27} and specifically in conjugation with the CPR algorithm.^{28,29}

The activation energies, calculated with the CPR algorithm, were sufficiently close to the experimental value. For example, the energy barrier for the solvated PT reaction involving three interconnecting water molecules was 14.87 kcal mol⁻¹ (compared to the experimental value, $E_a \approx 11$ kcal mol⁻¹). The PT reaction trajectories reveal that the transition state is highly strained and involves a supramolecular structure in which fluorescein and the interconnecting water molecules are covalently bonded together and the protons are shared between neighboring oxygens. This indicates that the PT reaction on the surface is semi- or fully concerted, never stepwise. A similar mechanism is assumed to be operative on the surface of proteins and explains how PT reactions between adjacent sites exposed to water can be so efficient.

Methods

Conjugate Peak Refinement. The approach used for obtaining the MEP by CPR² is summarized in Chart 1. Initially, we ran a MD simulation of fluorescein (oxyanion state, with hydrogen on the distal oxygen, Flu-COOH in Chart 2) in water. The MD methodology is reported below. The simulated cell contained 1 fluorescein molecule, 973 water molecules, and a single Na⁺ ion to keep the system neutral.

The MD trajectory consisted of 1000 conformations. Transient conformations from the MD trajectory were extracted for calculation of the MEP based on the number of water molecules that interconnected the donor and acceptor (2, 3, or 4). The selection of transient conformations was random otherwise. A single conformation was used for each CPR calculation. The coordinates of fluorescein and the participating water molecules were used for the calculations. The proton attached to the carboxylate was either retained on the distal oxygen (Flu-COOH in Chart 2) or relocated to the proximal one (Flu-COHO in

Chart 2). The whole system was then subject to energy minimization, using the adopted basis Newton Raphson (ABNR) algorithm, until no change in the potential energy was observed. The same procedure was repeated after placing the hydrogen on the oxyanion oxygen to create the product state. These two minimum energy states were used as an input to the CPR calculation, together with one or two intermediates that were created by manually modifying the location of one or two protons along the reaction coordinates. CPR trajectories could not be obtained without the inclusion of such intermediates. The refined trajectories, however, were independent of the initial conformation of the intermediate states, as the whole MEP is optimized with the CPR algorithm. The CPR calculation was carried out until the smallest fractional energy change was less than 10⁻⁵ kcal mol⁻¹. If convergence was obtained, then the system was further refined by allowing a larger number of line minimizations between saddle points. It should be noted, however, that this step had a minor (<0.01 kcal mol⁻¹) effect on the calculated activation energy.

All calculations were performed with the computer program CHARMM³⁰ version 31a1. The energies were calculated with the SCC-DFTB functional²³ as implemented in CHARMM.²⁴ The convergence criterion for each self-consistent field cycle was set to 10⁻¹⁰ kcal mol⁻¹, and the SCC-DFTB electronic temperature was set to 500.

Definition of the Reaction Coordinate. The reaction coordinate in CPR is defined as

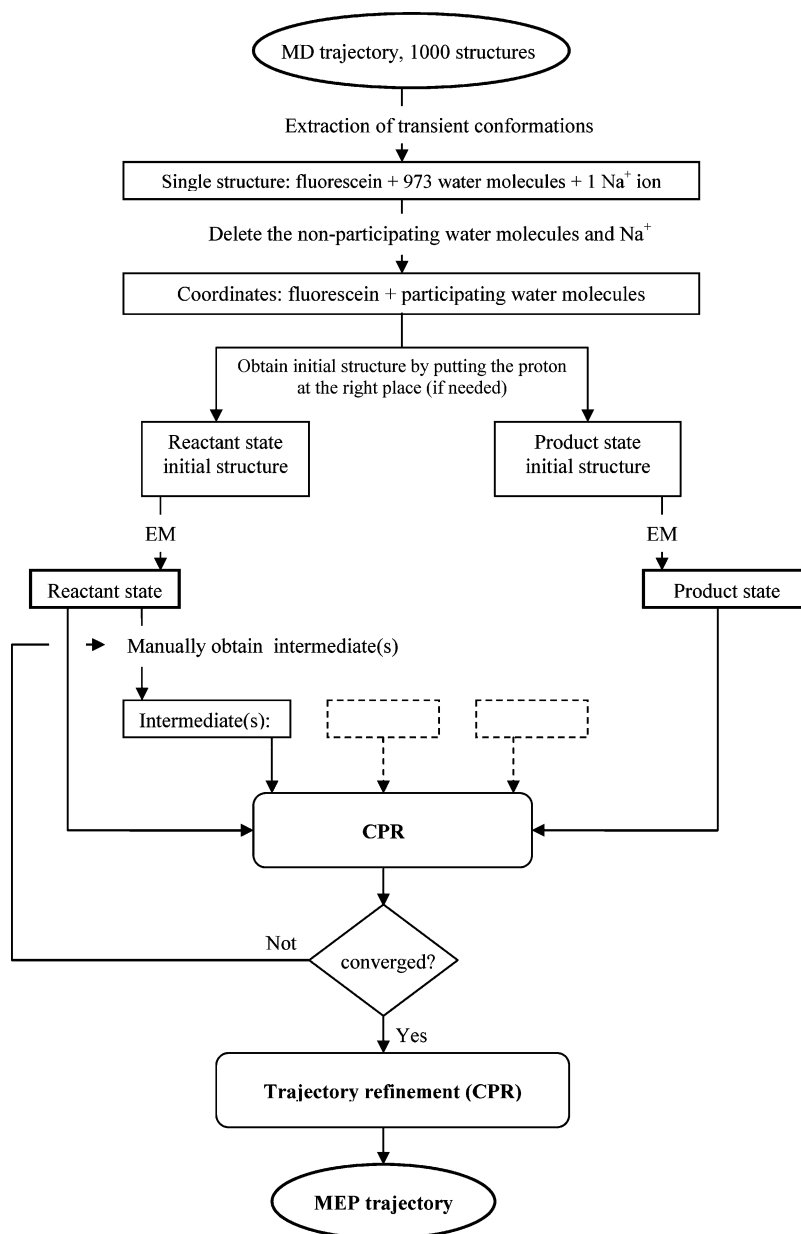
$$\lambda = \frac{\sum_{i=2}^N \{|\bar{\mathbf{x}}(i) - \bar{\mathbf{x}}(i-1)|\}}{\sqrt{3n}}$$

where N is the order of the point along the CPR trajectory, $\bar{\mathbf{x}}(i)$ are the coordinates of point i , and n is the number of atoms. As λ is a sum, it increases with each point, up to a maximum value for the product state. Throughout the paper, λ was normalized, so that $0 \leq \lambda \leq 1$.

Molecular Dynamics Simulations. The starting structure of the fluorescein molecule was modeled using the computer program GAMESS,³¹ using DFT with the 6-31Gd basis set. The wave functions were calculated using the B3LYP functional.^{32–35} The molecule was then put into a cubic box containing TIP3P model water,³⁶ leaving at least 1 nm between the solute and the edge of the box. One of the water molecules (selected randomly) was replaced by a sodium ion to keep the system neutral, leaving a total of 973 water molecules. Initially, the coordinates of the fluorescein were fixed to their initial positions, and the system was relaxed by 30 steps of conjugate gradient energy minimization (EM). The constraints on the fluorescein were set to 30.0 kcal mol⁻¹ Å⁻², and a new 30 step cycle of EM was run. After release of the constraints, the whole system was subject to 100 steps of EM with the ABNR algorithm. The system was gradually heated, from 50 to 300 K and equilibrated for 120 ps under constant temperature and pressure. Following the equilibration phase, the system was simulated for 1 ns, and the trajectory was saved and analyzed.

The time step between successive energy calculations was 2 fs. The nonpolar contribution to the energy was calculated up to a cutoff of 12 Å. The electrostatic interactions were calculated directly up to the same cutoff. Long-range electrostatic interactions were treated by the particle mesh Ewald algorithm³⁷ thereafter. The pressure was kept constant at 1 atm by use of the extended system algorithm³⁸ with a pressure piston

CHART 1



mass of 100 atomic mass units and a piston collision frequency of 10 ps^{-1} . Bonds to hydrogen atoms were constrained by the use of the SHAKE algorithm.³⁹

The CHARMM force field parameters for the fluorescein were set as follows. The partial charges were determined by fitting them to the electrostatic potential around the molecule using the Kollman/Singh method.⁴⁰ CHARMM atom types were set for each fluorescein atom, using the closest atom type in the Charmm22 force field.⁴¹ A similar approach was used previously in the simulations of fluorescein in water with the OPLS force field.¹

Geometry Optimization of Fluorescein. Geometry optimizations of different fluorescein species (Flu-COO⁻, Flu-COOH, and Flu-COHO, as presented in Chart 2) were performed in vacuo with the SCC-DFTB approximate functional in CHARMM. Reference calculations using semiempirical methods (AM1 and PM3) and DFT/B3LYP were performed with the GAMESS computer program.

The structures of the oxyanion species Flu-COHO and Flu-COOH were also optimized in a continuum solvent environment

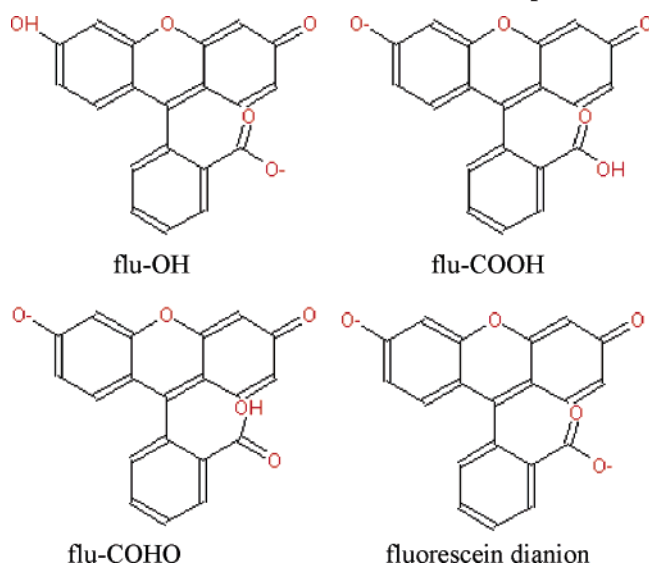
by use of the polarizable continuum model (PCM),⁴² the B3LYP DFT functional and the 6-31G+dp basis set.

The structures of the reactant state, transition state, and product state for the PT reaction of fluorescein with four water molecules were obtained by geometry optimization with B3LYP/6-31Gd in GAMESS.

Visual Presentation. Molecular figures were created by the use of the computer program VMD.⁴³

Results

Relative Energies of the Fluorescein Species. The CPR calculations, which were used to elucidate transition states along the PT mechanism, necessitate thousands of energy calculations. This makes the fluorescein system too large to be studied with B3LYP/6-31Gd or even with a much smaller basis set and Hartree-Fock (HF). For this reason, the calculations were performed with the DFT-SCCTB approximate density functional, which is orders of magnitude faster than HF calculations with a modest basis set. Before such calculations are performed,

CHART 2: Mono- and Dianionic Fluorescein Species^a

^a Top: Flu-OH (left), Flu-COOH (right). Bottom: Flu-COHO (left), Dianion Fluorescein (right). The single anionic fluorescein molecule can exist in three Conformations. One conformation, with a charged carboxylate (Flu-OH), is the most stable in water (and the least stable in vacuo). The two oxyanion species differ in the location of the proton on the carboxyl moiety. The proton can be located on each of the two carboxylate oxygens, which are not symmetric in relation to the supporting structure. We denote the oxyanion fluorescein species as Flu-COOH (where the hydrogen is distal to the molecule's center of mass) and Flu-COHO (where the hydrogen is proximal to it).

it should be verified that the approximate functional is sufficient for this study.

To assess whether SCC-DFTB is sufficiently accurate to be used for the current study, we calculated the gas-phase energies of the monoanion fluorescein species (Flu-OH, Flu-COOH, and Flu-COHO; see Chart 2), comparing the results obtained by the semiempirical methods (AM1 and PM3) and DFT calculations. The DFT calculations were performed either with the approximate density functional theory (DFT) functional SCC-DFTB or with the commonly used B3LYP hybrid functional. The latter was used with two basis sets: 6-31Gd and 6-31G+dp. The results are given in Table 1, where we referred to the energy differences between the monoanion fluorescein species.

As seen in the two upper rows of Table 1, the oxyanion species (Flu-COOH and Flu-COHO) are more stable than Flu-OH in vacuo, regardless of the calculation method. This is in contrast to the fully solvated conditions, where the carboxylate species is known from experiments to be more prevalent. The variation between the energies of the oxyanion and carboxylate forms is over-exaggerated when semiempirical methods are used, leading to energy differences as high as 16 kcal mol⁻¹, indicating that the semiempirical methods are not suitable for this study. However, the similarity between the values obtained with SCC-DFTB and B3LYP calculations using the largest basis set (6-31G+dp) is fairly good, indicating that this functional is sufficiently accurate for our calculations. In the case of the energy difference between the oxyanion and carboxylate species, the SCC-DFTB value is actually closer to the B3LYP/6-31G+dp calculation than B3LYP/6-31Gd.

Before calculating the MEP for the PT reaction, it was necessary to decide whether the hydrogen atom is more likely to be located on the oxygen proximal or distal to the fluorescein center of mass (i.e., on Flu-COHO or Flu-COOH). For this reason, we calculated the difference between the energies of these two oxyanion species. These energy differences are

displayed in the lowest row in Table 1, which shows that the Flu-COHO species is more stable, regardless of the calculation method. Yet, the energy difference between the two oxyanion species is quite small, accounting for ~2 kcal mol⁻¹. To verify if Flu-COHO is also more stable in solvent, the energy difference between the two oxyanion species was calculated using B3LYP/6-31G+dp, and the solvent environment was approximated with PCM.⁴² The values are presented in the table. Under these conditions, the energy difference between the two oxyanion species was as small as 1kT, i.e.,

$$E(\text{Flu-COOH}) - E(\text{Flu-COHO}) = 0.7 \text{ kcal/mol}$$

This indicates that both species can be present in solution. Therefore, both were considered as reactants throughout this study.

Proton Transfer through a Single Water Molecule. We used the CPR algorithm, in conjugation with the SCC-DFTB QM potential, to obtain PT trajectories in systems involving fluorescein and one or more water molecules. In all cases, the initial (proton on the donor, Flu-COOH or Flu-COHO) and final (proton on the acceptor, Flu-OH) fluorescein structures were obtained by rigorous energy minimization. The CPR algorithm starts by interpolating between the structures of the donor and acceptor states, thereby creating an initial crude trajectory. Structures along the crude trajectory often do not represent real structures; the reaction trajectory makes sense only after refinement. Depending on the coordinates of the initial and final states, structures along the initial trajectory may include free (i.e., nonbonded) atoms or atoms whose electron clouds significantly overlap. The relative energies of such structures are much higher (hundreds of kcal mol⁻¹) than the energies of the donor and acceptor states. Furthermore, when the wave functions of such structures are calculated (to obtain the corresponding energies) they may be impossible to converge if the structure is too erratic. In such cases, the CPR simulation crashes. To overcome this obstacle, we introduced one or more intermediates as part of the input to the CPR algorithm, based on the chemistry of the reaction (for the simulation setup, see Chart 1). This prevented the generation of too oddly shaped structures along the initial line interpolation, which is now carried out between the reactant, intermediates, and product state (i.e., reactant state → intermediate 1 → intermediate 2 ... → product state). The introduced intermediates will not be a part of the output CPR trajectory, as all of the intermediate points along the trajectory are refined by the CPR procedure.

In the following sections, we give atomistic details of the intramolecular PT reaction on fluorescein, as calculated using CPR. When describing the resulting CPR trajectories, we present the initial and final structures and the transition state (TS) following the CPR simulation. To compare the calculations to the experiment, we also calculate the activation energy for the whole PT process as $E_a = E_{\text{TS}} - E_{\text{REACTANT}}$.

The simplest model on which PT can be studied with fluorescein involves a single interconnecting water molecule. It should be stated that according to previous calculations the reaction is likely to involve 2–5 water molecules.¹ However, we include the donor–water–acceptor study case for the sake of methodological consistency. The minimum energy conformation of such a system prior to the PT reaction, as obtained by energy minimization, is displayed in Figure 1A. The (carboxylate OH)–HO–(oxyanion OH) distances are 2.73 and 4.01 Å, respectively. (For the O–H distances, see Figure S1 in the Supporting Information.) The distance between the water molecule and the acceptor is too large to enable the PT reaction

TABLE 1: Gas-Phase Energies of Fluorescein Species^a

calculated property	energy (kcal mol ⁻¹)				
	AM1	PM3	SCC-DFTB	B3LYP/6-31Gd	B3LYP/6-31G+dp
$E(\text{Flu-COOH}) - E(\text{Flu-OH})$	16.2	14.5	2.7	5.4	3.9
$E(\text{Flu-COHO}) - E(\text{Flu-OH})$	17.5	16.4	4.9	7.6	6.0
$E(\text{Flu-COOH}) - E(\text{Flu-COHO})$	1.3	2.0	2.2	2.2	2.1

^a Zero point energy corrections are not included.

without the motion of the heavy atoms of the system. Yet, we were able to obtain a trajectory of the reaction, as shown in Figure 1. The PT reaction starts with the proton moving from the donor to the water molecule (Figure 1B). This motion is accompanied by a slight movement of the acceptor oxygen toward the water molecule. The proton is not entirely relocated on the water molecule; i.e., it does not create an independent H_3O^+ species. Rather, it is shared between the donor oxygen of the fluorescein and the oxygen of the water (Figure 1B). As the reaction continues, the other proton attached to the water molecule (the one which is proximal to the acceptor) moves toward the oxyanion moiety, and the acceptor oxygen moves toward the water molecule, creating a supramolecular structure that corresponds with the transition state (Figure 1C). Finally, the bonds along the transition state break, leaving the proton on the acceptor (Figure 1D). The remainder of the simulation deals with the relocation of the water which moves to the vicinity of the charged carboxylate moiety (Figure 1, frames E–G). The activation energy, $17.2 \text{ kcal mol}^{-1}$, is due to the creation of the highly strained supramolecular species that is shown in Figure 1C.

Figure 2 shows the energy profile of the reaction. As seen in the figure, there are two saddle points. The first corresponds with the formation of the strained transition state conformation seen in Figure 1C. The relocation of the water molecule brings the system to a local energy minimum, which can be seen in Figure 1E. The location of the hydrogen on the acceptor O–H bond separates the local minimum energy state, as shown in Figure 1E from the final state, as shown in Figure 1G. The pathway that leads from the local minimum (Figure 1E) to the final state involves a second transition state (Figure 1F) whose energy is $3.9 \text{ kcal mol}^{-1}$ higher than that of the preceding the local minimum. This second transition state is due to the need to reorient the proton on the acceptor from its position as in Figure 1E to its position as in Figure 1G.

The strained quasi-stable state, as presented in Figure 1C, could not be achieved without internal flexibility of the dye molecule. The fluorescein flexes its oxyanion oxygen and the nearby carbons around the water molecule, creating a supramolecular system that involves all atoms in the system. The energy of the saddle point is $17.2 \text{ kcal mol}^{-1}$ higher than that of the reactant, in qualitative agreement with the experimental value ($E_a \approx 11 \text{ kcal mol}^{-1}$).

Proton Transfer through Two Water Molecules. MD simulations of fluorescein in water indicated that the shortest paths between the donor oxygen (of the carboxylate) and the acceptor oxygen (the oxyanion) involve 2–5 interconnecting water molecules.¹ It is therefore unlikely that the reaction in solvent proceeds via a single water molecule; there will be at least one more water molecule between the donor and the acceptor. For this reason, we ran CPR simulations with few water molecules present between the donor and the acceptor moieties.

Two PT trajectories were calculated for the reaction involving fluorescein and two water molecules, one with Flu-COOH as a reactant and the other with Flu-COHO. (For the definition of

fluorescein species, see Chart 2.) The resulting trajectories were very similar. In both cases, the PT process was concerted, and the transition state corresponded with a supramolecular structure involving all atoms in the system. The reactant (Flu-COHO), transition state, and product are displayed in Figure 3. Prior to the reaction, the water molecules are arrayed between the donor and the acceptor, creating a pathway of hydrogen-bonded oxygens (Figure 3A). The distances between neighboring oxygens are $2.73\text{--}2.81 \text{ \AA}$, as in bulk water. Upon formation of the supramolecular transition state (Figure 3B) the O–O distances shortened to $2.41\text{--}2.47 \text{ \AA}$, enabling PT. For the O–H distances, see Figure S2 in the Supporting Information. This proximity between the oxygen atoms is comparable with that of the Zundel ion, which is an essential component of the Grothuss PT mechanism. A comparison of the structures in Figures 3A and 3B reveals that the interconnecting water molecules had to reorient themselves closer to each other and to the donor and acceptor oxygens to form the transition state. The donor and acceptor oxygens of fluorescein, however, hardly move. This is in contrast to PT when a single water molecule is involved (Figure 1). Yet, the calculated activation energies (Flu-COHO, $16.9 \text{ kcal mol}^{-1}$, and Flu-COOH $16.6 \text{ kcal mol}^{-1}$) are quite similar to the reaction involving one water molecule ($17.2 \text{ kcal mol}^{-1}$; for a summary of the energies of activation, see Table 3).

The energy profile of the reaction is displayed in Figure 4. The reaction has only a single saddle point, which corresponds with the strained supramolecular structure seen in Figure 3B. The conformation of the O–H bond in the product state, pointing outward (Figure 3C), is similar to that in the local energy minimum obtained along the trajectory with a single water molecule (Figure 1E). Thus, this reaction avoids a second phase needed to reorient and stabilize the product state (in contrast with the mechanism presented in Figure 1).

Proton Transfer Via Three Interconnecting Water Molecules. The initial structure for the intramolecular reaction involving three water molecules is presented in Figure 5A. The three water molecules form a hydrogen-bonded network that connects the donor and acceptor oxygens. This network is not arrayed linearly as in the case of the reactions with one or two water molecules. The distance between the acceptor oxygen and the closest water molecule is 2.76 \AA , while its distance to the next is as large as 3.47 \AA . Due to the nonlinear organization of the three water molecules, the energy barrier for the PT reaction is higher in the case of three water molecules, rising to $22.2 \text{ kcal mol}^{-1}$. The energy profile is similar to the one seen in Figure 2 for the reaction with a single water molecule; i.e., there are two transition states (results not shown).

The transition state is shown in Figure 5B, and the product in Figure 5C. Reorganization of the waters occurs just prior to the formation of the product state (as seen when the structures in Figures 5B and 5C are compared). In the product state, two of the three water molecules solvate the carboxylate, while the other is hydrogen-bonded to one of them but not to the acceptor oxygen (Figure 5C). Please note that in this case the negatively

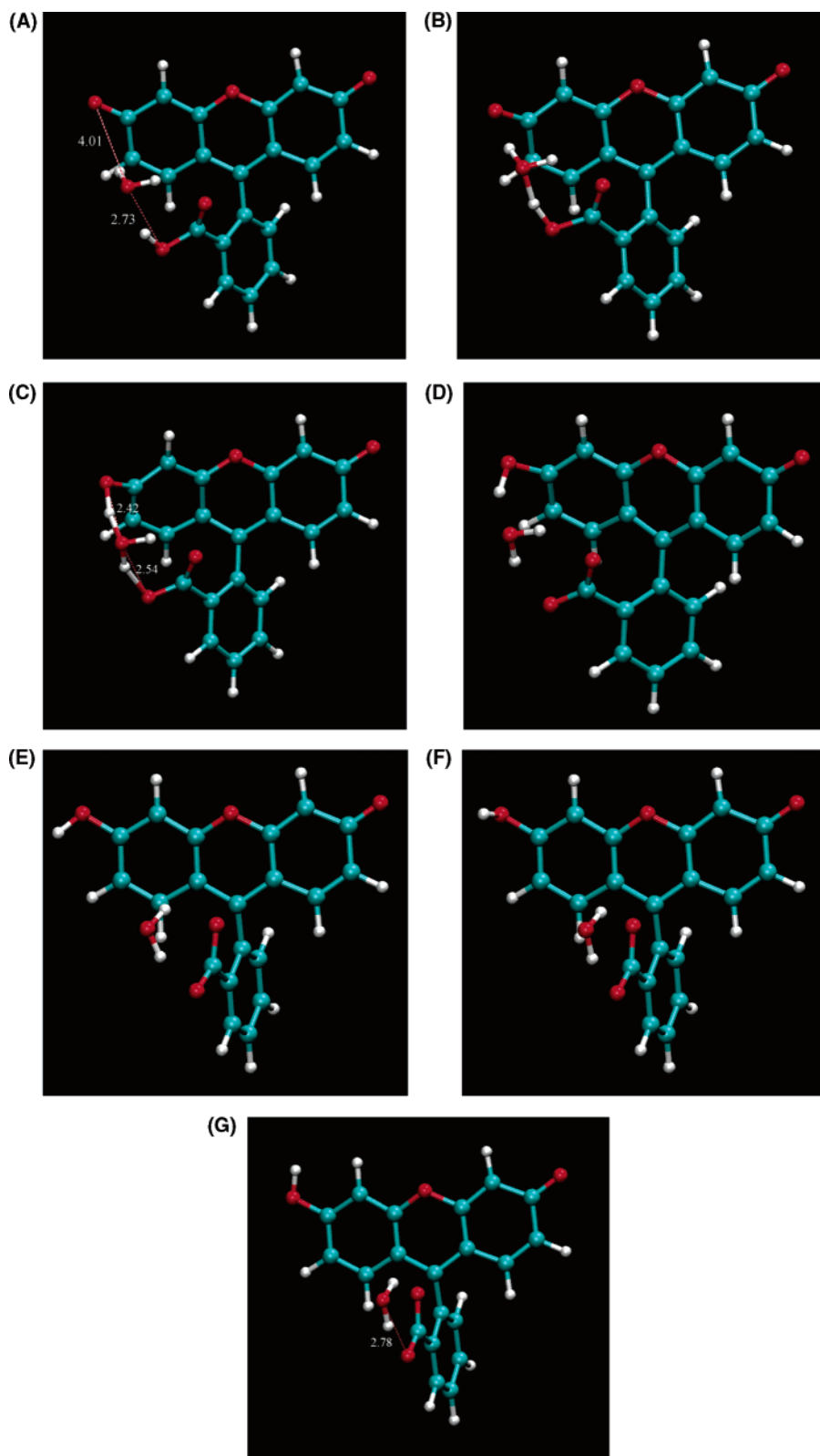


Figure 1. Intermediate points along the trajectory of the PT pathway on fluorescein, from the carboxylate to the oxyanion, through a single water molecule. Some O—O distances are presented. For the O—H distances, Figure S1 of the Supporting Information. (A) Flu-COOH, structure at energy minimum. The distance between the donor oxygen and the water is 2.73 Å. The distance between the acceptor oxygen and the water molecule is 4.01 Å. (B) The first step in the PT reaction. The hydrogen is shared between the water molecule and the donor oxygen. The acceptor oxygen starts moving toward the water molecule. (C) Structure at the highest energy saddle point. The fluorescein molecule twists, creating a supermolecular structure with the water. The donor—water—acceptor oxygen distances are 2.54 and 2.42 Å. (D) Flu-OH, immediately after the collapse of the supramolecular structure. The structure shown in this frame is still unstable due to the high charge density on the fluorescein moiety. (E) Flu-OH, in the intermediate point which corresponds with the local energy minimum along the reaction path. Note the location of the hydrogen on the acceptor O—H bond, pointing left. (F) The second saddle point along the reaction path. Note the location of the hydrogen on the acceptor O—H bond, pointing forward (G) Flu-COO[−], structure at energy minimum. Note the location of the hydrogen on the O—H bond, pointing upward. The distance between the donor oxygen and the water is 2.78 Å.

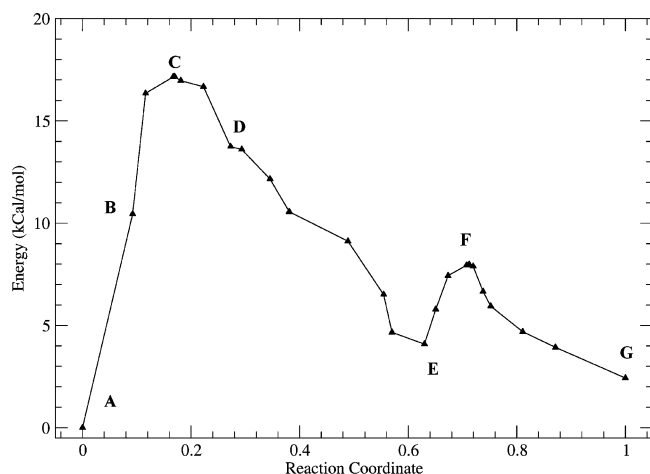


Figure 2. Energy profile of the intramolecular proton-transfer reaction for fluorescein, with a single water molecule. The energy values are relative to the energy of the reactant (Flu-COOH). The reaction coordinate is based on the structural difference between points along the CPR trajectory and the reactant structure (see Methods). It was scaled between 0 for the reactant and 1 for the product. The letters A–G correspond to the structures in Figures 1A–G.

charged site is stabilized by two water molecules while the other site is hydrogen-bonded to one water molecule.

Proton Transfer in a Solvated System. When the number of water molecules in the system is increased to four and the system is minimized with respect to its energy, the optimized structures have only two interconnecting water molecules, and the other two solvate the PT system. The reactant, transition state, and product along the PT pathway are shown in Figure 6 (and also in Figure S4 in the Supporting Information). All water molecules form a hydrogen-bonded network, involving the oxygens of the donor and the acceptor moieties. This hydrogen-bonded network lasted throughout the reaction. The activation energy for the reaction was $16.3 \text{ kcal mol}^{-1}$, similar to the reactions with two interconnecting water molecules and no solvating waters. (For a summary of the activation energies, see Table 2.) The energy profile involved a single saddle point and was similar to the one shown in Figure 4.

Obtaining PT trajectories for a system involving more than four water molecules is a challenging task. Due to the large number of degrees of freedom, such systems converge, if ever, very slowly. In fact, most of the simulations including >4 water molecules did not converge, due to the formation of highly strained intermediates, whose wave functions could not be obtained. Yet, by running dozens of simulations, using various initial conditions, we managed to calculate two PT trajectories with more than four water molecules. The reaction pathway for our largest system, fluorescein and nine water molecules, is displayed in Figure 7. Three of the nine water molecules interconnected the donor and the acceptor. Another three formed the solvation shell for the interconnecting pathway. The rest solvated the fluorescein oxyanion oxygen that did not participate in the PT reaction and did not change their locations during the reaction. As in the case involving three interconnecting water molecules, the water molecules that participated in the PT reaction needed to relocate their positions to enable the formation of the transition state. This solvent reorganization leads to the formation of the supramolecular transition state as seen in Figure 7B. The transition state is stabilized by the solvation shell of the interconnecting water molecules, leading to an energy barrier of $14.3 \text{ kcal mol}^{-1}$. This energy barrier is $\sim 8 \text{ kcal mol}^{-1}$ smaller than the energy barrier for PT with three interconnecting water molecules and no solvation shell. More-

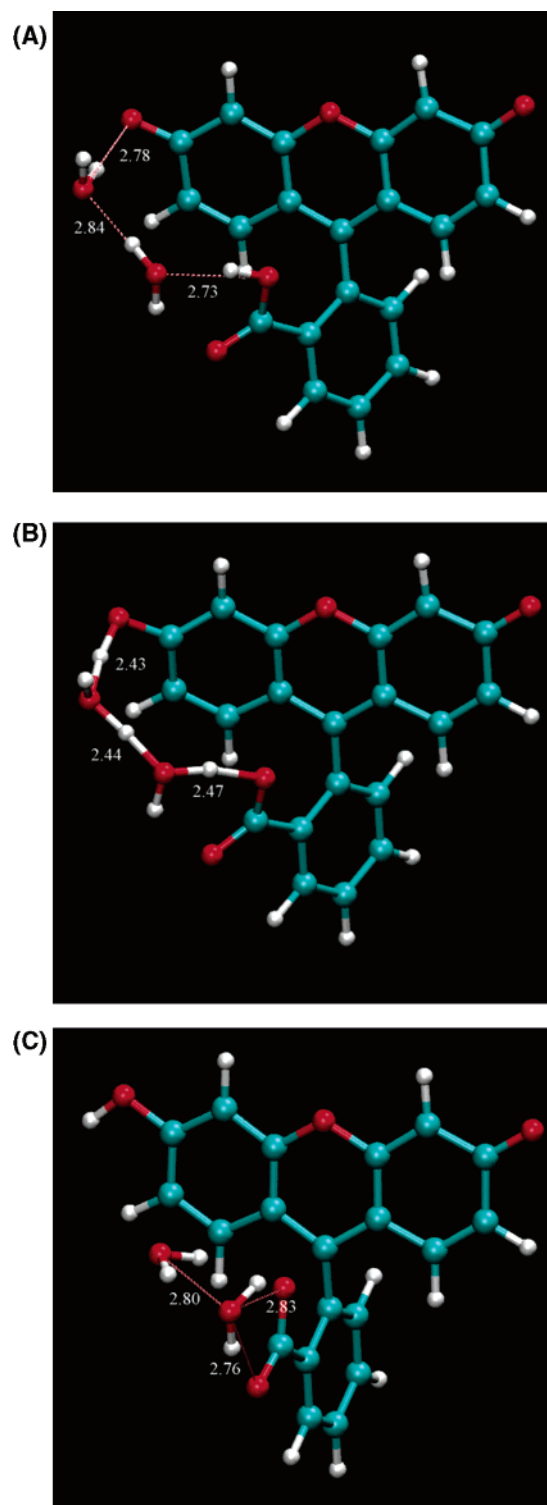
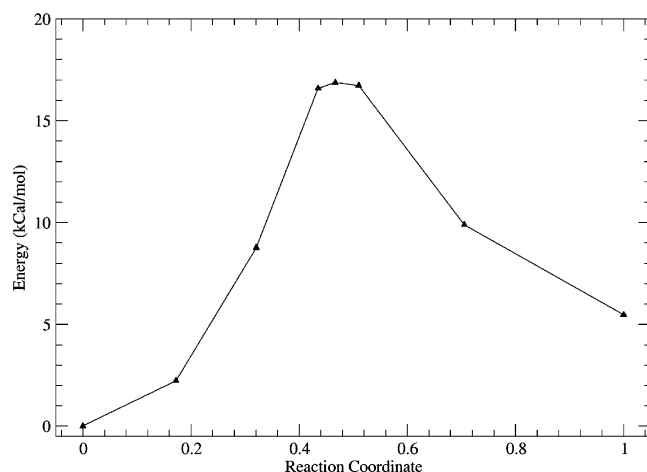


Figure 3. Stationary points along the fluorescein carboxylate to oxyanion PT pathway through two interconnecting water molecules. Some O–O distances are indicated. For O–H distances, see Figure S2 in the Supporting Information. (A) Flu-COOH, structure at energy minimum. The donor–water–water–acceptor oxygen distances are 2.73, 2.84, and 2.78 Å, respectively. (B) Structure at the transition state. The donor–water–water–acceptor oxygen distances are 2.47, 2.44, and 2.43 Å, respectively. (C) Flu-COO[−], structure at energy minimum. The distances between the carboxylate oxygens and the oxygen of the nearest water molecule oxygen are 2.76 and 2.83 Å. The water–water oxygen distance is 2.80 Å.

over, the calculated energy barrier is very similar to the experimentally estimated one ($\sim 11 \text{ kcal mol}^{-1}$), which indicates that the PT reaction is likely to involve three water molecules

TABLE 2: Relative Energies of Fluorescein Species, Calculated with DFT B3LYP/6-31+Gdp, with the Solvent Represented by PCM^a

calculated property	energy (kcal mol ⁻¹)
$E(\text{Flu-COOH}) - E(\text{Flu-OH})$	3.2
$E(\text{Flu-COOH}) - E(\text{Flu-COO}^-)$	3.9
$E(\text{Flu-COOH}) - E(\text{Flu-COOH}^-)$	0.7

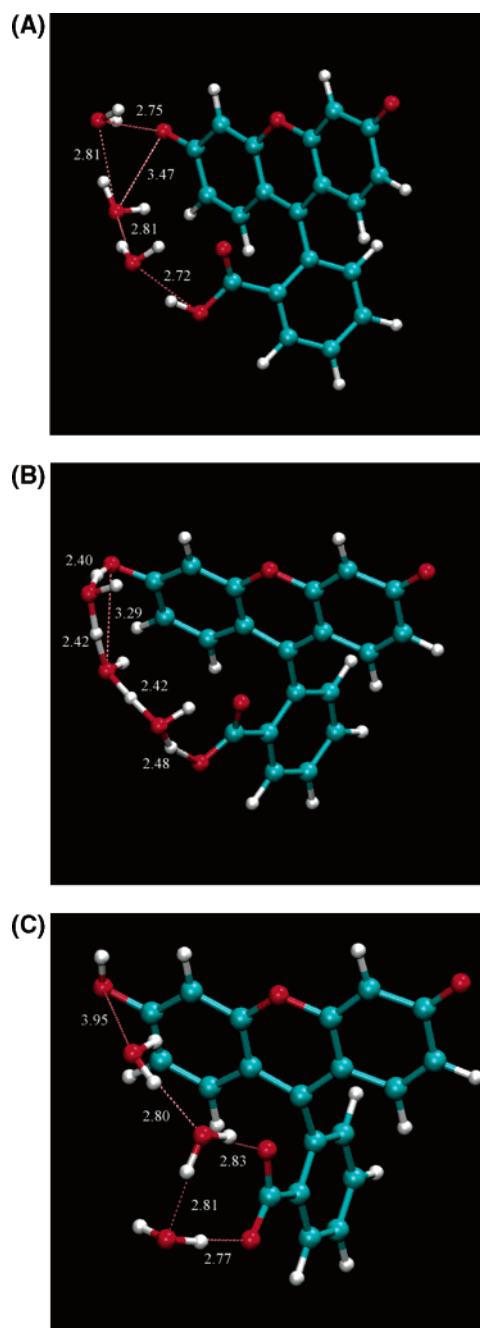
^a Zero point energy corrections are not included.**Figure 4.** Energy profile of the intramolecular proton-transfer reaction for fluorescein, with two water molecules. The energy values are relative to the energy of the reactant, which is presented in Figure 3A. The definition of the reaction coordinate is given in the Methods.

in a fully solvated system. Apparently, when three water molecules are involved in a PT reaction in the absence of solvating water molecules, the presence of the solvation shell significantly lowers the energy barrier by maintaining hydrogen bonds with the interconnecting water molecules.

The trajectory obtained for a system with seven water molecules (two interconnecting and five solvating molecules) was similar to the trajectories shown in Figures 3 and 5, where two water molecules interconnected the donor and the acceptor. Surprisingly, the energy barrier was as high as 19.3 kcal mol⁻¹, which is higher than the energy barrier without solvating water. This energy barrier indicates that the solvation shell may work against the intramolecular PT reaction. Apparently, in the system with fluorescein and seven water molecules, the local organization of the solvating water destabilizes the transition state. Taking into account the activation energies for the reactions with seven and nine water molecules, we conclude that the solvation shell can work either in favor of or against the PT reaction. Due to the prevalence of the donor to acceptor interconnecting water networks,¹ the PT pathways that will be selected are those in which the solvation shell aids in lowering the energy barrier.

The Transition State as Calculated with the B3LYP Functional. To compare between the data gathered by the use of hybrid (B3LYP) and approximate (SCC-DFTB) DFT functionals, the structures of the reactant (FLU-COOH), transition state and product for the PT reaction in the presence of four water molecules were re-optimized using B3LYP/6-31Gd. The energy barrier for the PT reaction was calculated as 10.9 kcal mol⁻¹, very close to the experimental value. When the zero point energy (ZPE) correction was taken into account, the energy barrier was lower: $E_a = 5.6$ kcal mol⁻¹.

The B3LYP transition state is presented in Figure 8. Overall, this transition state is similar to the one obtained with the use of SCC-DFTB (Figure 6B). However, when the transition state

**Figure 5.** Stationary points along the fluorescein carboxylate to oxanion PT pathway through three interconnecting water molecules. (A) Flu-COOH, structure at energy minimum (before PT). (B) Structure of the transition state. (C) Flu-COO⁻, structure at energy minimum (after PT). For O-H distances, see Figure S2 of the Supporting Information.

is calculated with B3LYP, there is no proton located on the donor molecule. Apparently, the proton first moves from the donor to the nearest water, and then a supramolecular structure is created between the acceptor and the interconnecting water molecules. In spite of the apparent difference between the structures shown in Figures 6B (and Figure S4 in the Supporting Information) and Figure 8, the variation between the transition states calculated by use of the different functionals is rather small. The difference should be attributed to the distance between the donor oxygen and the nearest hydrogen, which is 1.43 or 1.61 Å when calculated with SCC-DFTB and B3LYP/6-31Gd, respectively.

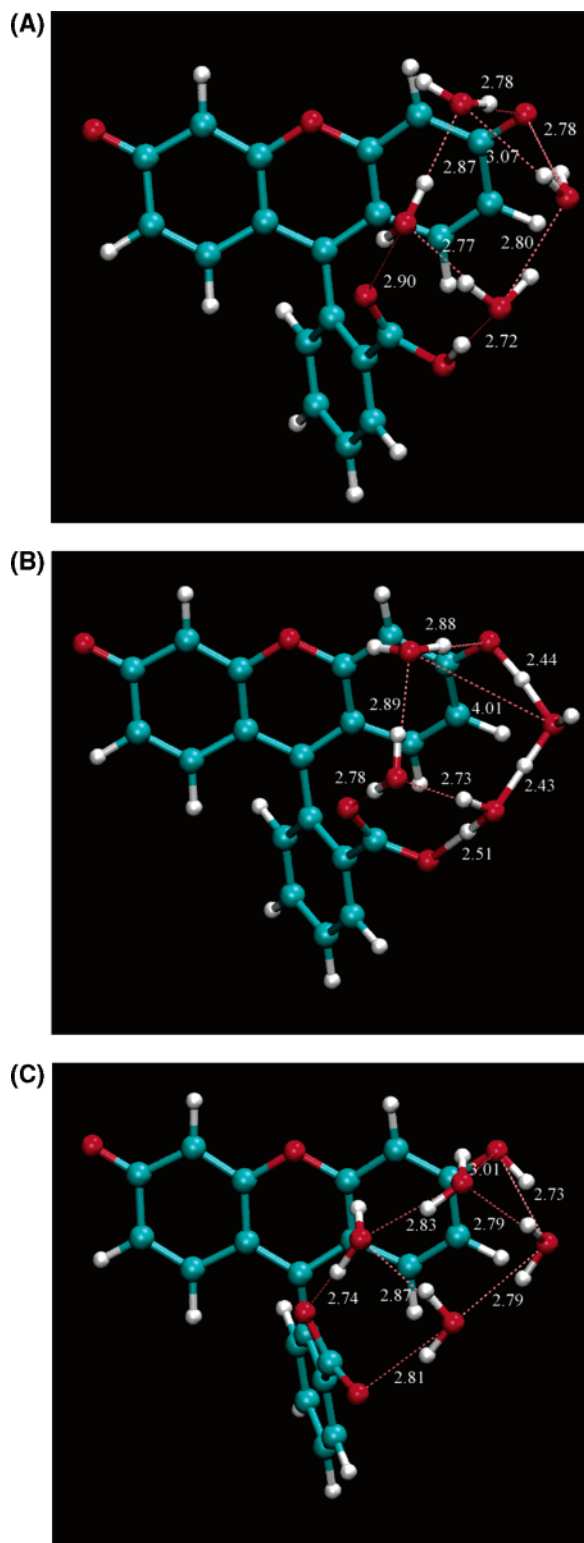


Figure 6. Stationary points along the fluorescein carboxylate to oxyanion PT pathway with four water molecules. Two water molecules interconnected the donor and acceptor; the other two solvated the participants of the reaction. (A) Flu-COOH, structure at energy minimum (before PT). (B) PT intermediate. (C) Flu-COO⁻, structure at energy minimum (after PT). For O-H distances, see Figure S4 of the Supporting Information.

Discussion

Activation Energies. The activation energies of all of the reactions, as calculated by the use of the CPR algorithm, are summarized in Table 3. All CPR calculations were performed

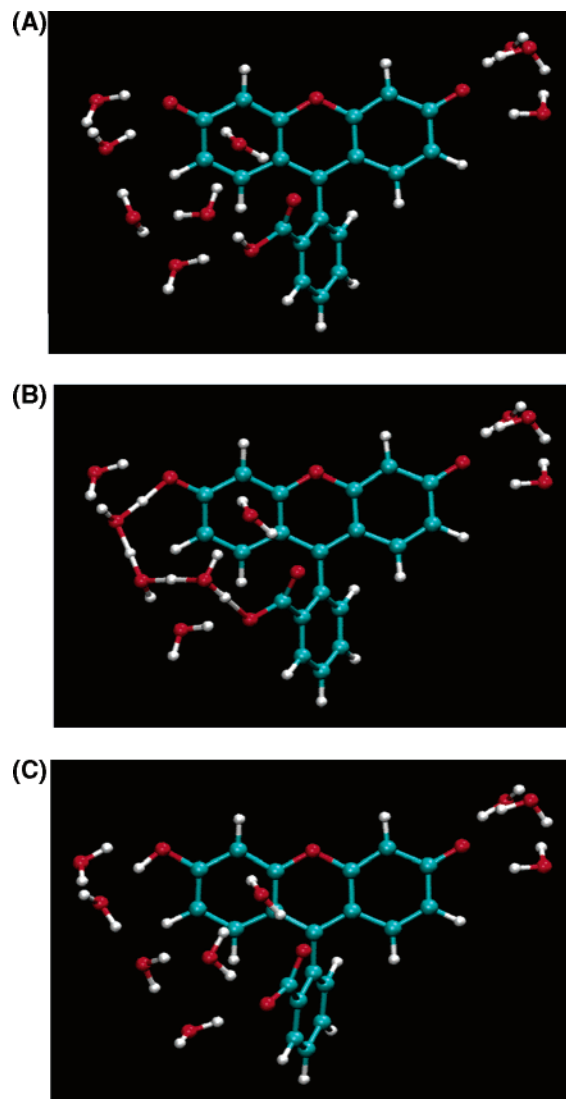


Figure 7. Stationary points along the fluorescein carboxylate to oxyanion PT pathway through three interconnecting water molecules in the presence of six solvating molecules. (A) Flu-COOH, structure at energy minimum (before PT). (B) Transition state. (C) Flu-COO⁻, structure at energy minimum (after PT).

with the SCC-DFTB approximate density functional. In one case, PT in a system that involved four water molecules, the structures of the donor state, acceptor state, and transition state were re-optimized using a more elaborated DFT functional (B3LYP/6-31Gd). The B3LYP/6-31Gd energy was quite similar to the SCC-DFTB energy (as seen in Table 3).

The calculated energy values are very close to the experiment, with the lowest SCC-DFTB activation energy (14.3 kcal mol⁻¹), ~3 kcal mol⁻¹ above the experimentally estimated value. Unfortunately, the relative uncertainty of the experimental value is rather high; it may well be in the 3 kcal mol⁻¹ range. The similarity between the experimental and calculated values therefore indicates that the PT mechanism, as seen in the CPR calculation (or geometry optimization with B3LYP), is highly probable.

Proton Transfer: Concerted, Semiconcerted, or Stepwise?

Two reaction mechanisms may describe the PT reaction. In the stepwise mechanism the proton will propagate in discrete steps along the train of hydrogen bonds. In the concerted reaction, however, the passage will be in a single event in which the donor site loses its proton, the acceptor gains one, and the interconnecting water molecules shuttle a proton among them.

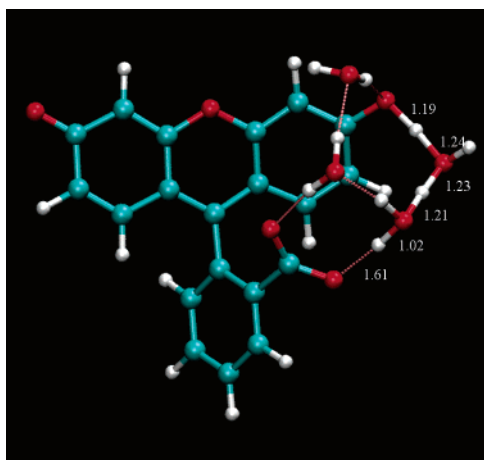
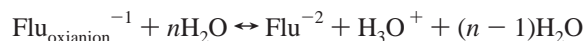


Figure 8. Transition state for proton transfer on the surface of fluorescein through two interconnecting water molecules and in the presence of two solvating molecules, as calculated using B3LYP/6-31Gd. The O–H distances along the proton-transfer pathway, from the donor through the water to the acceptor (as listed on the figure) are 1.61, 1.02, 1.21, 1.23, 1.24, and 1.19 Å. The corresponding O–O distances are 2.62, 2.44, and 2.42 Å (not shown). The carboxylate moiety, all water molecules, and the acceptor oxygen are hydrogen-bonded to each other.

In practice, both stepwise and concerted mechanisms were assumed prior to running the CPR simulations, and a corresponding set of structures was subject to CPR treatment. When the set of structures that had been used as an input for the CPR simulation involved an intermediate that corresponded with a stepwise mechanism, it led to one of two consequences. Either the resulting pathway was concerted or there was no resulting pathway (i.e., the system failed to converge). To demonstrate this, let us consider a stepwise mechanism, where a proton is first transferred from the donor to the water molecule, forming fluorescein dianion and H_3O^+ , as presented in Figure 9. This structure was used as an intermediate state in the input of the CPR simulation. The resulting pathway, however, revealed a concerted PT reaction, in which all protons are located between their neighboring oxygens (as seen in Figure 5C).

Although no independent H_3O^+ or H_2O_5^+ species were observed at any point along the CPR trajectories it does not indicate that the formation of such species is impossible but that once formed the intramolecular PT reaction will not be operative. When H_3O^+ or H_2O_5^+ is formed, there can be two consequences:

I. The proton returns to the donor oxygen, i.e.,



II. The proton diffuses from the protonated into the bulk water by the familiar Grotthuss mechanism.

The transfer of a proton from the donor to the bulk (rather than to the acceptor) was evident in 50% of the PT reactions on fluorescein.¹ The MEP that leads to PT into the bulk cannot be studied using CPR in conjugation with any QM potential, since the product state (including a protonated water species in this case) should be energy-minimized prior to the CPR simulation. Such minimization will always lead back to the donor state, which is much more stable than a state that contains a protonated species such as H_3O^+ (i.e., the reaction will proceed as in I).

To estimate the energy of the intermediate of PT from the carboxylate moiety of fluorescein to the bulk water, we optimized a structure that involves fluorescein dianion and an

H_3O^+ species by a constrained geometry optimization. The structure of this intermediate is shown in Figure 10. Its energy, as calculated with B3LYP/6-31Gd, is 12.4 kcal mol⁻¹ above that of the donor state. The activation energy is thus 1.6 kcal mol⁻¹ higher than that of the transition state seen in Figure 8, as calculated by the same level of theory (10.9 kcal mol⁻¹). The activation energy should be referred to as an upper bound for the reactant \rightarrow intermediate activation energy, since the system cannot be fully optimized when constraints are present. We therefore conclude that the formation of a free protonated water species (Figure 10) is almost as probable as the formation of the supramolecular PT intermediate (Figure 8B) but does not evolve into an intramolecular PT process. Instead, the proton may rebind to the donor or escape to the bulk water, leaving the dianion species behind. In a fully hydrated system the H_3O^+ ion, formed next to the donor site, can rapidly propagate to the bulk by the Grotthuss mechanism.

Without the formation of a protonated water species, a fully stepwise mechanism is not possible. The reaction may therefore proceed either in a concerted mechanism, where all protons move together, or in a semiconcerted mechanism, where some, but not all, protons move simultaneously along the PT pathway. Examination of the CPR trajectories reveals that in the transition states all protons were shared between their neighboring oxygens. This indicates a concerted PT pathway.

When only a single water molecule was present, PT was neither concerted nor stepwise. The protons moved together but not simultaneously: The second proton moved toward the acceptor before the first proton already moved to the water molecule (Figures 1B and 1C). We refer to this combined mechanism as semiconcerted. Similarly, when the reaction was studied with B3LYP/6-31Gd, the transition state indicated that the proton-transfer reaction is semiconcerted (Figure 8). The proton moves to the nearest water molecule, and then all protons in the interconnecting PT network move together. For the DFT–SCCTB structure (Figure 6 and Figure S4 in the Supporting Information) the donor oxygen to nearest hydrogen distance is 1.43 Å, compared with the other O–H distances which are 1.08–1.25 Å. This also suggests that a semiconcerted mechanism is the preferred pathway.

The finding that the PT was concerted or semiconcerted but never stepwise is in agreement with other stretched systems involving water molecules. In an early study by Scheiner,⁴⁴ multiple PTs were studied on a system of cationic oligomers of water: H_7O_3^+ and $\text{H}_{11}\text{O}_5^+$. In the pentamer state, the TS involved the partial transfer of one proton. The transfer of a second proton was coupled to the completion of the transfer of the first one. A few years later, Yamabe and co-workers studied the double PT reaction in a formamidine–water system, i.e., $\text{H}_2\text{N}-\text{CH}=\text{NH} + \text{H}_2\text{O} \rightarrow \text{H}_2\text{O} + \text{NH}=\text{CH}-\text{NH}_2$.⁴⁵ The TS was a supramolecular structure, and both the proton of the water and one of the two protons attached to the nitrogen moved simultaneously. Later studies involved PT reactions inside proteins, modeled at increasing levels of complexity. Liang and Lipscomb⁴⁶ studied the PT reaction in the active site of carbonic anhydrase II, a popular system for studies of PT in proteins. The active site was modeled as a system of four ammonia molecules (representing imidazole moieties), five water molecules, and a zinc ion. The reaction proceeded from a Zn^{2+} -bound water molecule to an ammonia acceptor, representing His64. PT was found to be concerted. Later studies with larger systems confirmed that the PT reaction in the enzyme is indeed concerted or semiconcerted.^{27,47,48} Interestingly, Isaev and Scheiner⁴⁷ found that solvating water molecules raise the energy

TABLE 3: Energy Barriers Calculated for the CPR Calculated Trajectories^a

number of waters		reactant conformation	ΔE	remarks
interconnecting	solvating			
2		Flu-COOH	16.6	
2		Flu-COHO	16.9	
3		Flu-COOH	22.2	The pathway was initiated as concerted.
3		Flu-COOH	22.2	The pathway was initiated as stepwise but was concerted following CPR.
2	2	Flu-COOH	16.3	
			10.9 (5.6)	The energy barrier was recalculated using DFT-B3LYP with the 6-31Gd basis set. The value in parentheses is the energy barrier after ZPE correction
3	6	Flu-COOH	14.3	All water molecules within 3.0 Å of the -OH oxygen or oxyanion oxygen were included.
2	5	Flu-COHO	19.3	All water molecules within 3.0 Å of the donor or acceptor oxygens were included.
experimental value			~11	Reference 1

^a All values are in kcal mol⁻¹. Unless otherwise stated, all calculations were performed using the SCC-DFTB approximate density functional.

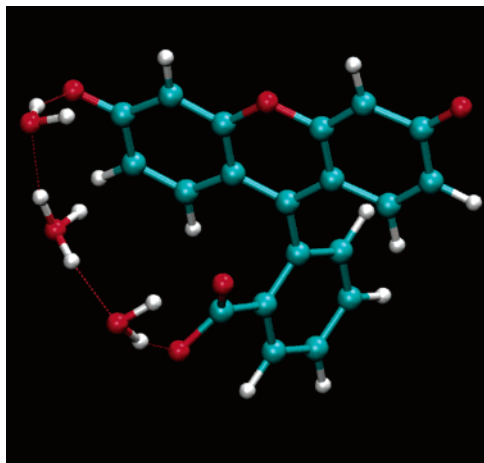


Figure 9. Intermediate, as used for the initiation of the CPR refinement for the PT reaction with three water molecules. When the CPR trajectory is optimized, no such intermediate was present, and the transition state was similar to the one shown in Figure 5B.

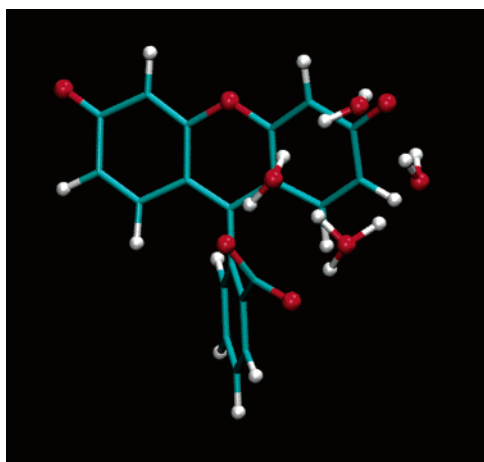


Figure 10. Structure of a system with doubly charged fluorescein, H₃O⁺, and three water molecules as obtained from geometry optimization with constraints. A rotation of the protonated water molecule may lead to PT into the bulk water.

barrier for the PT reactions, as in the fluorescein system with two interconnecting and five solvating water molecules. Yet, this was attributed to stabilizing the positive charge that accompanies the proton, which is not the case in fluorescein. Rather, it is the need to reorient those solvating water molecules that raises the energy barrier.

The fluorescein system has a lot in common with PT on the protein surface. The donor–acceptor distances are similar, and the reaction proceeds under the surrounding Coloumb cage, as on the surface of proteins.¹⁷ This leads to the conclusion that

PT on the protein is not likely to be stepwise. Due to the many degrees of freedom for PT reactions on proteins, a fully concerted mechanism does not seem to be likely, and thus we conclude that PT on the protein surface should be semiconcerted.

Contribution of the Surrounding Solvent and Temperature. Through the use of CPR simulations we were able to obtain the PT MEP whose activation energies were similar to the experiment. The resulting PT trajectories shed light on the atomistic mechanism of the reactions. However, it should be reminded that the CPR trajectories, as studied here, have their limitations. First, we were only able to study PT reactions in the presence of a small number of water molecules, not in a fully solvated system. Second, the resulting trajectories follow the reaction on the MEP, which corresponds to a temperature of 0 K. Therefore, in the following section, we shall discuss the potential effect of solvation and elevated temperature. Due to computational limitations, which prevent us from performing more elaborate calculations, we limit our discussion to the qualitative level.

In the case of the reaction where three water molecules interconnected the donor and acceptor moieties, addition of solvating waters lowered the energy barrier by stabilizing the transition state structure (Figure 7B). The solvating water molecules remained in their initial configuration as the supramolecular structure was formed. Since molecules in the first solvation shell did not reorient, we do not expect the inclusion of the second and higher solvation shells in the calculations to have a significant effect. This leads to the conclusion that solvent effects were properly approximated in our treatment, at least inasmuch as we aim at studying the configuration of transition states.

Solvent effects, however, should be considered when the energies of the reactant and the product states are calculated. In vacuo, the charge on the carboxylate moiety (Flu-OH in Chart 2) makes it less stable than the two other charged species, i.e., Flu-COOH and Flu-COHO. The opposite is true in an aqueous environment, where the water molecules that surround the carboxylate moiety, COO⁻, stabilize the carboxylate over the oxyanion state, whose resonative smeared charge does not attract water molecules in the same way. This leads to the conclusion that the activation energy may be lower in a complete aqueous environment, yielding the calculated values in Table 3 (without ZPE corrections) as upper limits for the activation energy of the reaction along the MEP.

Temperature effects (entropy and kinetic energy) are not so clear cut. When the PT reaction is studied at room temperature, the reactant and the water molecules have a plethora of conformations that they can adopt, and the formation of the exact minimum energy conformation (which corresponds to a temperature of 0 K) is unlikely. However, MD simulations show

that arrays of water molecules that interconnect the donor and acceptor oxygens are widely distributed.¹ As there are many conformations on which PT can proceed, the formation of reaction pathways such as those used in this study is in fact very probable. This leads us to conclude that the reaction trajectories at room temperature will be similar, but not identical, to those that were obtained through the use of the CPR algorithm.

Temperature effects can also be manifested in the zero point vibrational energy (ZPE). The ZPE difference between the reactant and the transition state may make the energy barrier different than the value along the MEP. Unfortunately, we are unable to take into account the ZPE with the current implementation of DFT–SCCTB in CHARMM. When the transition state was obtained with the B3LYP functional (Figure 8), the ZPE correction was found to lower the activation energy by as much as 5.0 kcal mol⁻¹. Yet, this ZPE correction is due to the vibrations of the atoms in vacuo, and the correction in a solvated system is not expected to lower the activation energy by a similar amount. In a solvated system, the presence of the water molecules, which border the reaction pathway, will restrain the vibrations of the reactant, transition, and product states. Consequently, the ZPE correction will be smaller, and the activation energy in solution will be higher than the ZPE-corrected value calculated in vacuo (5.6 kcal mol⁻¹).

Concluding Remarks

PT between groups on the molecular surface, through the solvent, is prevalent in many systems, including fluorescein and its derivatives, proteins, and membranes. In these PT reactions, surface groups exchange protons through the solvent under the influence of an electrostatic field. The ability of a few water molecules to generate a PT pathway had been well established. In the present study we showed that the local ordering of water molecules on the surface enabled the PT reactions to take place. The PT reaction was operative both in vacuo and in solvent, and the calculated activation energies were in good agreement with the experiment. The similarity between PT on the surface of fluorescein, as we studied, and on the protein surface indicates that transition states, such as obtained here, are likely to be observed on the surface of PT proteins such as bacteriorhodopsin, cytochrome c oxidase, or photosynthesis reaction center. The semiconcerted PT mechanism renders PT reactions between adjacent sites exposed to water highly efficient in spite of high activation energies, as the intramolecular PT intermediates cannot lead to PT reaction from the donor to the bulk water.

Acknowledgment. This study was supported by the United States–Israel Binational Science Foundation (Grant No. 2002129). The collaboration between the authors was further supported by the Minerva Fellowship and by a short-term fellowship from the European Molecular Biology Organisation. R.F. greatly acknowledges the Colton Foundation for supporting him through the Colton Fellowship.

Supporting Information Available: Intermediate points along the trajectory of the PT pathway on fluorescein, from the carboxylate to the oxyanion, through a single water molecule, two water molecules, and three water molecules and through two water molecules with two solvating water molecules. This material is available free of charge via the Internet at <http://pubs.acs.org>.

References and Notes

(1) Mezer, A.; Friedman, R.; Noivirt, O.; Nachliel, E.; Gutman, M. *J. Phys. Chem. B* **2005**, *109*, 11379.

- (2) Fischer, S.; Karplus, M. *Chem. Phys. Lett.* **1992**, *194*, 252.
- (3) Macdonald, P. M.; Seelig, J. *Biochemistry* **1988**, *27*, 6769–6775.
- (4) Mitchell, P. *Nature* **1961**, *191*, 144.
- (5) Konstantinov, A. A. *J. Bioenerg. Biomembr.* **1998**, *30*, 121.
- (6) Wikstrom, M.; Morgan, J. E.; Verkhovsky, M. I. *J. Bioenerg. Biomembr.* **1998**, *30*, 139.
- (7) Lanyi, J. K. *Biochim. Biophys. Acta* **1993**, *1183*, 241.
- (8) Neutze, R.; Pebay-Peyroula, E.; Edman, K.; Royant, A.; Navarro, J.; Landau, E. M. *Biochim. Biophys. Acta* **2002**, *1565*, 144.
- (9) Edmonds, B. W.; Luecke, H. *Front. Biosci.* **2004**, *9*, 1556.
- (10) Feniouk, B. A.; Cherepanov, D. A.; Junge, W.; Mulikidjanian, A. Y. *FEBS Lett.* **1999**, *445*, 409.
- (11) Okamura, M. Y.; Feher, G. *Annu. Rev. Biochem.* **1992**, *61*, 861.
- (12) Namslauer, A.; Brzezinski, P. *FEBS Lett.* **2004**, *567*, 103.
- (13) Adelroth, P.; Brzezinski, P. *Biochim. Biophys. Acta* **2004**, *1655*, 102.
- (14) Papa, S.; Capitanio, N.; Capitanio, G. *Biochim. Biophys. Acta* **2004**, *1655*, 353.
- (15) Branden, G.; Gennis, R. B.; Brzezinski, P. *Biochim. Biophys. Acta* **2006**.
- (16) Gutman, M.; Nachliel, E. *Annu. Rev. Phys. Chem.* **1997**, *48*, 329.
- (17) Friedman, R.; Nachliel, E.; Gutman, M. *Biochim. Biophys. Acta* **2005**, *1710*, 67.
- (18) Gutman, M.; Nachliel, E.; Friedman, R. *Biochim. Biophys. Acta* **2006**.
- (19) Gutman, M. *Methods Biochem. Anal.* **1984**, *30*, 1.
- (20) Cukier, R. I. *Biochim. Biophys. Acta* **2004**, *1655*, 37.
- (21) Checover, S.; Marantz, Y.; Nachliel, E.; Gutman, M.; Pfeiffer, M.; Tittor, J.; Oesterheld, D.; Dencher, N. A. *Biochemistry* **2001**, *40*, 4281.
- (22) Marantz, Y.; Einarsdottir, O. O.; Nachliel, E.; Gutman, M. *Biochemistry* **2001**, *40*, 15086.
- (23) Elstner, M.; Porezag, D.; Jungnickel, G.; Elsner, J.; Haugk, M.; Frauenheim, T.; Suhai, S.; Seifert, G. *Phys. Rev. B* **1998**, *58*, 7260.
- (24) Cui, Q.; Elstner, M.; Kaxiras, E.; Frauenheim, T.; Karplus, M. *J. Phys. Chem. B* **2001**, *105*, 569.
- (25) Elstner, M.; Cui, Q.; Munih, P.; Kaxiras, E.; Frauenheim, T.; Karplus, M. *J. Comput. Chem.* **2003**, *24*, 565.
- (26) Elstner, M.; Frauenheim, T.; Suhai, S. *J. Mol. Struct. (THEOCHEM)* **2003**, *632*, 29.
- (27) Smedarchina, Z.; Siebrand, W.; Fernandez-Ramos, A.; Cui, Q. *J. Am. Chem. Soc.* **2003**, *125*, 243.
- (28) Bondar, A. N.; Elstner, M.; Suhai, S.; Smith, J. C.; Fischer, S. *Structure* **2004**, *12*, 1281.
- (29) Walewski, L.; Krachtus, D.; Fischer, S.; Smith, J. C.; Bala, P.; Lesyng, B. *Int. J. Quantum Chem.* **2006**, *106*, 636.
- (30) Brooks, B. R.; Bruccoleri, R. E.; Olafson, B. D.; States, D. J.; Swaminathan, S.; Karplus, M. *J. Comput. Chem.* **1983**, *4*, 187.
- (31) Schmidt, M. W.; Baldrige, K. K.; Boatz, J. A.; Elbert, S. T.; Gordon, M. S.; Jensen, J. H.; Koseki, S.; Matsunaga, N.; Nguyen, K. A.; Su, S.; Windus, T. L.; Dupuis, M.; Montgomery, J. A. *J. Comput. Chem.* **1993**, *14*, 1347.
- (32) Babu, Y. S.; Bugg, C. E.; Cook, W. J. *J. Mol. Biol.* **1988**, *204*, 191.
- (33) Becke, A. J. *Phys. Chem.* **1993**, *98*, 5648.
- (34) Becke, A. D. *J. Chem. Phys.* **1993**, *98*, 1372.
- (35) Lee, C. Y. W.; Parr, R. G. *Phys. Rev. B* **1988**, *37*, 785–789.
- (36) Jorgensen, W. L.; Chandrasekhar, J.; Madura, J. D.; Impey, R. W.; Klein, M. L. *J. Chem. Phys.* **1983**, *79*, 926.
- (37) Darden, T.; York, D.; Pedersen, L. *J. Chem. Phys.* **1993**, *98*, 10089.
- (38) Feller, S. E.; Zhang, Y. H.; Pastor, R. W.; Brooks, B. R. *J. Chem. Phys.* **1995**, *103*, 4613.
- (39) van Gunsteren, W. F.; Berendsen, H. J. C. *Mol. Phys.* **1977**, *34*, 1311.
- (40) Singh, U. C.; Kollman, P. A. *J. Comput. Chem.* **1984**, *5*, 129.
- (41) MacKerell, A. D.; Bashford, D.; Bellott, M.; Dunbrack, R. L.; Evanseck, J. D.; Field, M. J.; Fischer, S.; Gao, J.; Guo, H.; Ha, S.; Joseph-McCarthy, D.; Kuchnir, L.; Kuczera, K.; Lau, F. T. K.; Mattos, C.; Michnick, S.; Ngo, T.; Nguyen, D. T.; Prodhom, B.; Reiher, W. E.; Roux, B.; Schlenkrich, M.; Smith, J. C.; Stote, R.; Straub, J.; Watanabe, M.; Wiorkiewicz-Kuczera, J.; Yin, D.; Karplus, M. *J. Phys. Chem. B* **1998**, *102*, 3586.
- (42) Miertus, S.; Scrocco, E.; Tomasi, J. *Chem. Phys.* **1981**, *55*, 117.
- (43) Humphrey, W.; Dalke, A.; Schulten, K. *J. Mol. Graphics* **1996**, *14*, 33.
- (44) Scheiner, S. *J. Am. Chem. Soc.* **1981**, *103*, 315.
- (45) Yamabe, T.; Yamashita, K.; Kaminoyama, M.; Koizumi, M.; Tachibana, A.; Fukui, K. *J. Phys. Chem.* **1984**, *88*, 1459.
- (46) Liang, J. Y.; Lipscomb, W. N. *Biochemistry* **1987**, *26*, 5293.
- (47) Isaev, A.; Scheiner, S. *J. Phys. Chem. B* **2001**, *105*, 6420.
- (48) Cui, Q.; Karplus, M. *J. Phys. Chem. B* **2003**, *107*, 1071.